



A material recognition method for underwater application based on Micro Thermoelectric Generator

Changxin Liu^{a,*}, Baichuan Shan^a, Nanxi Chen^a, Jianhao Liu^a, Zhenghui Zhou^a,
Qingyong Wang^a, Yu Gao^a, Yunfei Gao^b, Zhitao Han^a, Zhijian Liu^b, Minyi Xu^a

^a Marine Engineering College, Dalian Maritime University, Dalian 116026, China

^b Navigation Training and Engineering Practice Center, Dalian Maritime University, Dalian 116026, China

ARTICLE INFO

Keywords:

Underwater material recognition
Heat Transfer
Thermal tactile
Thermoelectric effect
Micro Thermoelectric Generator

ABSTRACT

Many complex ocean conditions, such as low brightness and ultra-high-water pressure, hinder human exploration of the underwater world. Underwater material recognition technology is the key to exploring the underwater world as support. This paper proposes a theory of underwater material recognition based on the thermoelectric effect. Based on the above theory, a prototype is designed, and its performance under common marine conditions is tested. The results show that the prototype can accurately recognize three different types of typical materials, which are thermostatic animals, non-metal materials and metal materials within 2 s. The prototype has the advantages of accurate recognition, low cost, and easy maintenance. While various materials have complex surface morphology in the application, a flexible thermal conductive material proposed by this paper can enhance recognition accuracy. Through the experimental verification, a recognition device with a flexible contact surface made of flexible thermal conductive material has been more effective.

1. Introduction

The ocean, which occupies 71% of the earth, is still covered with a mysterious veil today, and the reason is inseparable from the particularity of the marine environment. Under the ocean, low brightness and ultra-high water pressure hinder human exploration of the underwater world. In order to explore the underwater world, it is extremely important to perform an accurate recognition of underwater materials. Material recognition is the key to exploring and utilizing the underwater world, which can be applied to underwater rescue, underwater salvaging, river bed analysis, underwater monitoring, underwater pipeline laying, waste disposal and building foundations analysis, etc. [1].

As shown in Fig. 1, material recognition technology has significant potential in ocean engineering applications. Similar to Fig. 1(a), the remote operated vehicle (ROV) and autonomous underwater vehicle (AUV) can get sensor information with a recognition device to recognize unknown objects. And the ideal recognition device is shown in Fig. 1(b). As shown in Fig. 1(c), the material recognition technology can be utilized to detect the thickness of the hull paint coating, which means that the detection of hull paint coating can be completed by robots. As shown

in Fig. 1(d)–(f), the material recognition technology can be utilized to recycle cultural relics, salvage wrecks, and capture marine organisms.

At present, there are two kinds of mature technologies in the field of material recognition. One is acoustic spectrum formant recognition technology [2], the other is optical underwater material recognition technology based on polarization imaging [3]. Both of them enable rapid and secure material recognition. The optical underwater material recognition has the advantage of high sensitivity, especially in distinguishing between metals and non-metals. However, due to the complexity of the underwater environment, the difficulty of extracting feature parameters increases. Besides the complex databases and procedures of these recognition techniques, the equipment has the disadvantages of being expensive, difficult to operate and maintain. Clearly, a low-cost, easy-operation and easy-to-maintain technique is required in the field of underwater recognition. Nowadays, underwater material recognition is only well established in the field of optics and acoustics. Although there is a thermal tactile recognition technique in the field of thermodynamics based on heat conduction theory, it is rarely applied underwater [4].

Thermal tactile recognition technology was first proposed by Katz [5]. According to Katz, the sensory perception of cold and hot was the

* Correspondence to: Department of Marine Engineering, Dalian Maritime University, Dalian, Liaoning Province, China.

E-mail address: liu_changxin@dlnu.edu.cn (C. Liu).

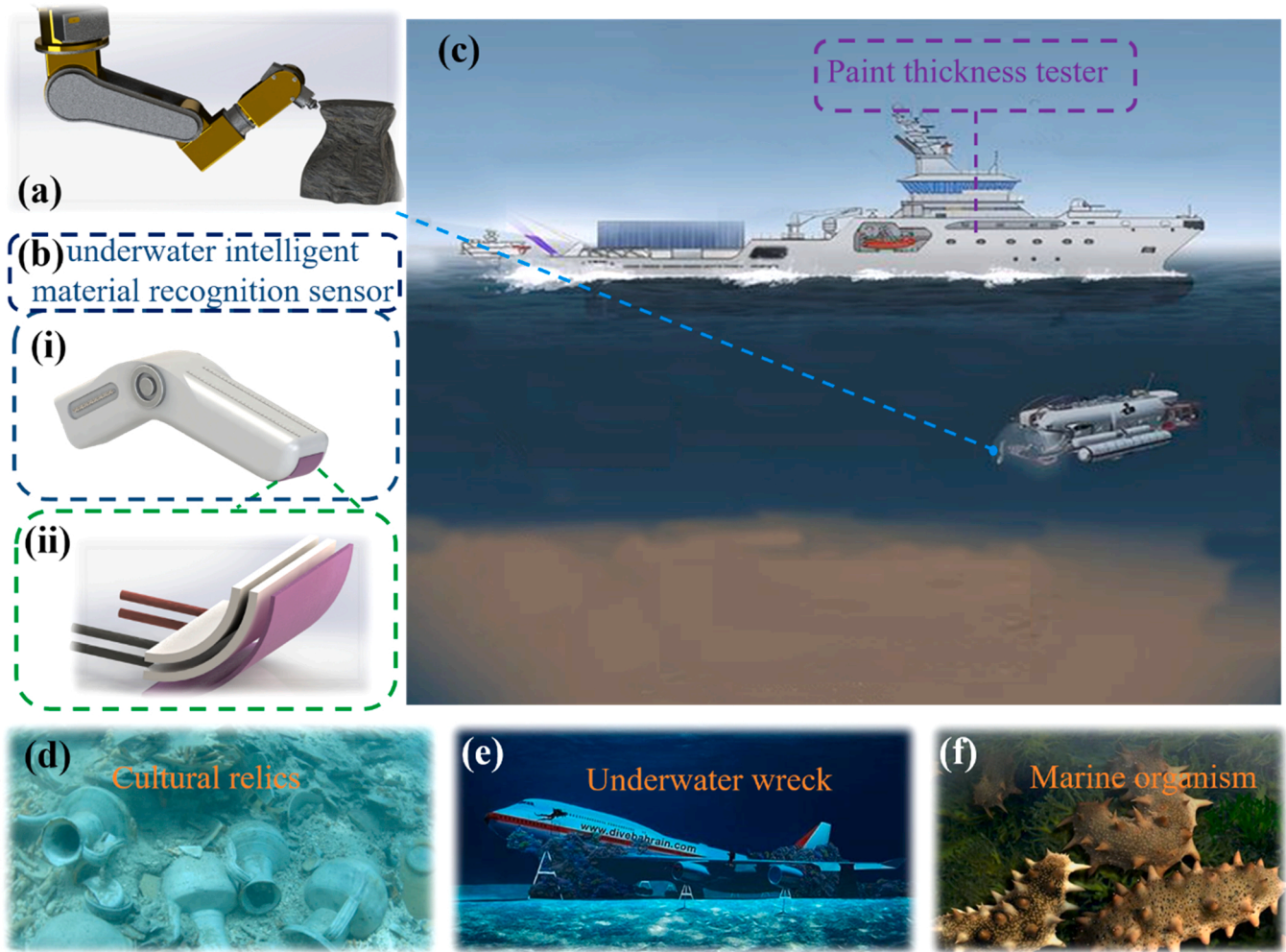


Fig. 1. Application prospect of material recognition device in ocean engineering typical manipulator with recognition device (b) i) recognition device, ii) contact-side magnification of recognition device (c) detect bottom of the hull (d) recycle relics (e) salvage wreck (f) grab marine organism.

key judgment factor in human's recognition of the materials contacted. Many researchers have focused on the subject of material recognition by imitating human senses. For example, Havenith found that the thermal conductivity of materials could directly affect the cold and hot felt by a human in contact with materials [6]. The research of Mills showed that when two types of materials contact each other, the temperature of the contact surface only depended on the inherent properties of the material if the size remained unchanged [7]. Sarda found that the size of the contact object could affect the temperature curve by experiments [8]. With the development of the theory, the researchers have designed prototypes to verify the recognition effect under the guidance of the theory.

Recently, factors such as pressure and thermal resistance have been considered by some researchers to improve recognition accuracy in the field of thermal tactile recognition [9]. Others have prioritized the design and data processing of the thermal tactile recognition device to improve recognition accuracy [10].

Based on the theory of thermal tactile technology and the previous research of our team in the field of Thermoelectric Generator (TEG) [11–17], a theoretical model for material recognition based on the thermoelectric effect of Micro Thermoelectric Generator (MTEG) is proposed in this paper. The theoretical model focuses on the MTEG voltage curves to realize material recognition. The MTEG voltage curves are easier to observe and have obvious characteristics. A prototype based on this theoretical model is proposed, which can recognize three typical material types underwater by comparing the voltage curves. The

prototype has the characteristics of small volume, high sensitivity, easy maintenance, low cost, and good adaptability. Moreover, in combination with the flexible contact surface, the recognition effect of the prototype is improved.

2. Theoretical model and prototype design

Fig. 2 shows the schematic diagram of heat transfer for the theoretical model. Based on the heat conduction theory, the thermal tactile recognition principle and MTEG functional principle, the heat conduction process of the theoretical model is shown in Fig. 2(a).

In application, the Heat source unit can be a human or a common lithium battery pack. However, to get ideal and stable recognition results in the experiment, the Peltier unit (PU), which can control temperature stably, is employed as the heat source unit. In order to maintain the stability of the PU temperature, the cooling unit is connected to the hot end of the PU to absorb the excess heat from it. The heat transfer power in the PU satisfies the following equation:

$$Q = I\pi_{PN} \quad (1)$$

π_{PN} represents the Peltier coefficient of the material; I represents the current, and Q represents the exothermic power of the PU.

Through a thermodynamically tight fit, the hot end temperature of the PU is the same as that of the MTEG as the PU operates steadily. The cold end temperature of PU is $t_{p,cool}$ and the hot end temperature of the

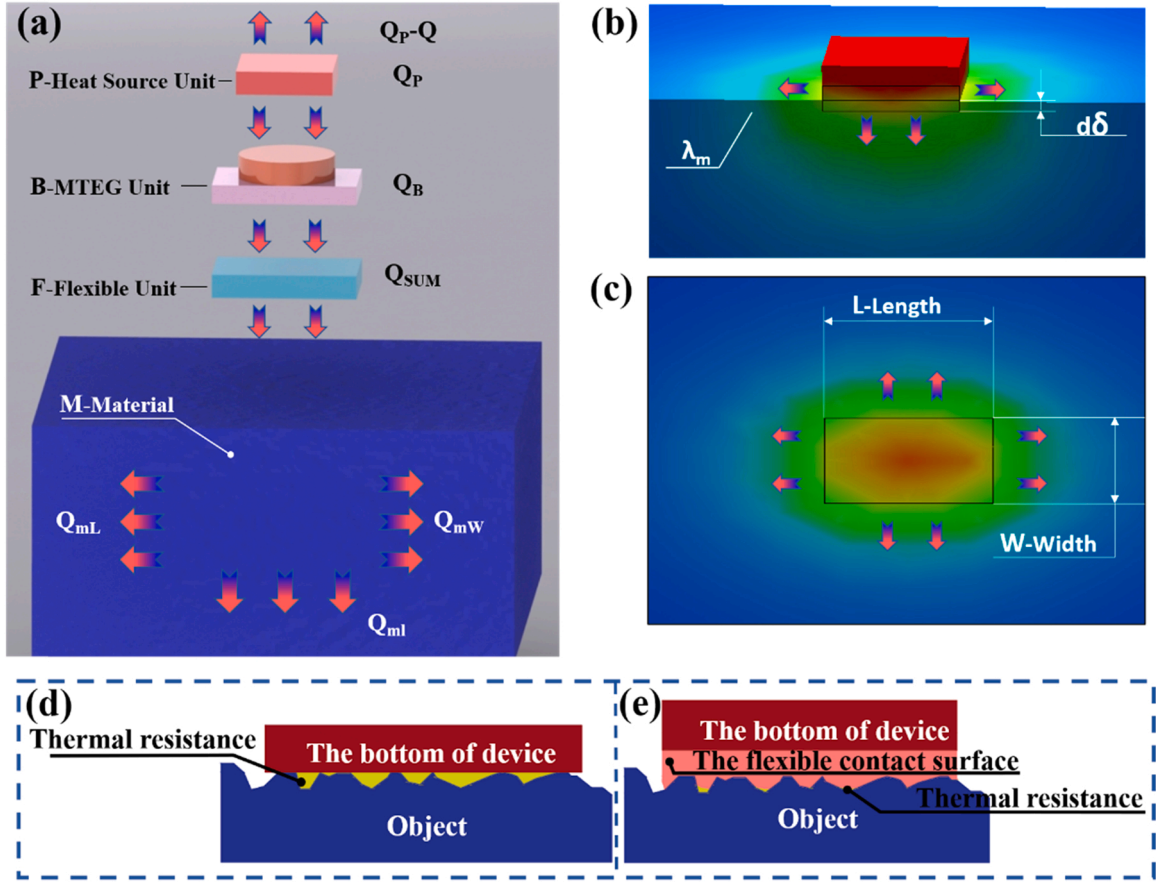


Fig. 2. Schematic diagram of heat transfer (a) heat conduction process (b) front view of MTEG Unit contacting Material (c) vertical view of MTEG Unit contacting Material (d) thermal resistance without flexible contact surface (e) thermal resistance with the flexible contact surface.

PU is $t_{P,hot}$ when the PU works stably. According to the second law of thermodynamics, the heat transfers from the hot end of the PU to the cold end of the PU, and the heat transfer power satisfies the equation:

$$Q_P = \frac{\lambda_P A_P (t_{P,hot} - t_{P,cool})}{\delta_P} \quad (2)$$

The subscript P represents PU, λ represents the thermal conductivity of the material, A represents the area of the thermal conductive layer, and δ represents the thickness of the thermal conductive layer.

Similarly, according to the second law of thermodynamics, the heat transfer power from the hot end of the MTEG unit to the cold end of the MTEG unit satisfies the equation:

$$Q_B = \frac{\lambda_B A_B (t_{B,hot} - t_{B,cool})}{\delta_B} \quad (3)$$

The subscript B represents the MTEG unit.

The cold end of the MTEG unit comes in contact with the object. Due to the volume difference between the MTEG unit and the object in application scenarios, it is assumed that the environment does not affect the heat transfer from the cold end of the MTEG unit to the contact surface. Once the heat is transferred to the contact surface, a part of the heat is transferred along the vertical direction of the contact surface as Fig. 2(b) shows. The other part is transferred along the parallel direction of the contact surface as shown in Fig. 2(c).

As shown in Fig. 2(b), the thickness of the thermal conductive layer on the contact surface is defined as infinitesimal, and $d\delta$ is utilized to denote it. The heat transfer of $d\delta$ satisfies the equation:

$$Q_m = \frac{\lambda_m A (t_{m1} - t_{m2})}{d\delta} \quad (4)$$

The subscript m represents the material of the object.

The transferred heat leads to elevating the temperature of the contact surface which means the temperature of the space $Ad\delta$ rises. Because of equation $M = \rho V$ and $V = Ad\delta$, the rising temperature satisfies the equation[18]:

$$\Delta T_m = \frac{Q_m}{\rho_m c_m A d\delta} = \frac{\lambda_m (t_{m1} - t_{m2})}{\rho_m c_m (d\delta)^2} \quad (5)$$

ρ represents the density, c represents the specific heat capacity, and M represents the mass.

As Fig. 2(b) shows, when the contact surface is heated, the heat is transferred along both the vertical direction and parallel direction of the contact surface inside the material.

The heat transfer power equation of the infinitesimal heat conduction layer $d\delta$ perpendicular to the contact surface is similar to the Eq. (4). The temperature difference $(t_{m1} - t_{m2})$ in the equation can be replaced by ΔT_m :

$$Q_{m1} = \frac{\lambda_m A \Delta T_m}{d\delta} \quad (6)$$

The rising temperature of $Ad\delta$ is:

$$\Delta T_{m1} = \frac{Q_{m1}}{\rho_m c_m A d\delta} = \frac{\lambda_m \Delta T_m}{\rho_m c_m (d\delta)^2} \quad (7)$$

The heat transfers in the parallel direction of the contact surface as shown in Fig. 2(c). The rectangular heat conduction layer is taken as the subject, with the length of L and the width of W .

The heat transfer power equation along the vertical direction of L is:

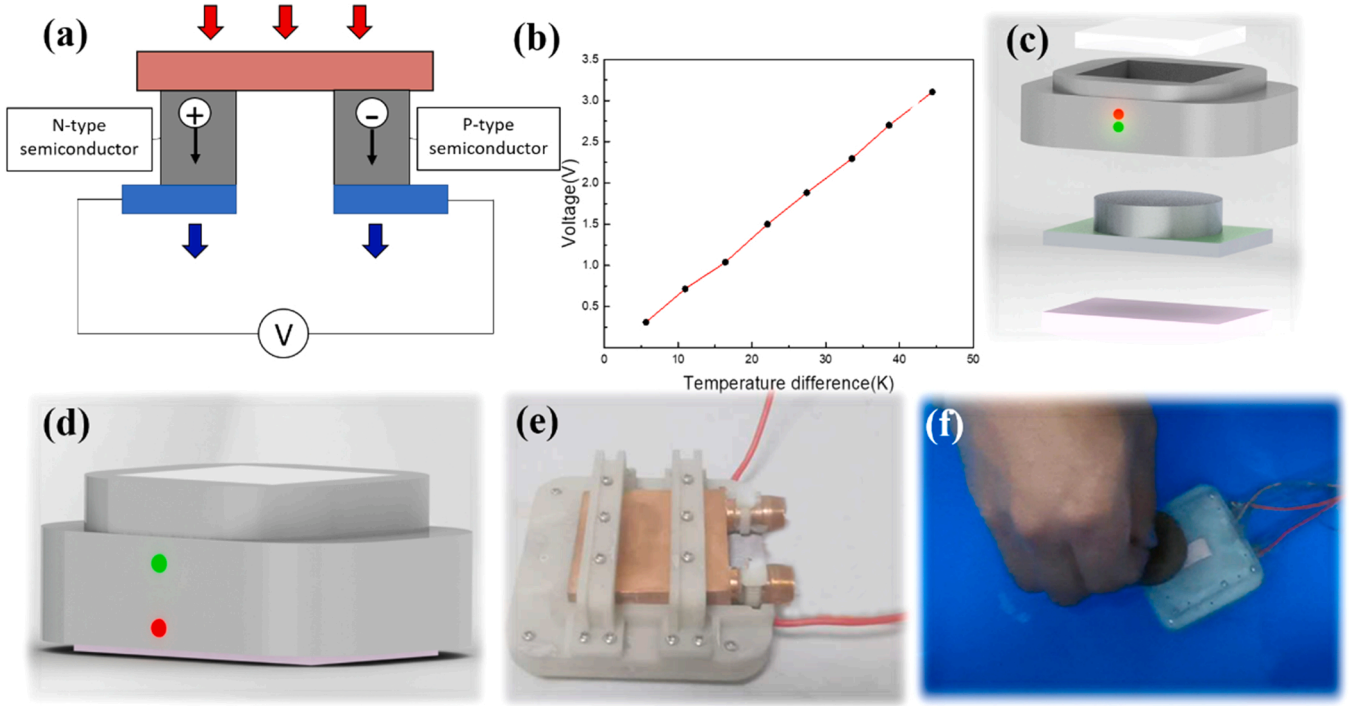


Fig. 3. The prototype and working principles (a) thermoelectric effect (b) temperature difference-voltage diagram (c) explosive view of prototype (d) prototype model (e) real photograph of prototype (f) prototype in working.

$$Q_{mL} = \frac{\lambda_m A_L \Delta T_{m1}}{d\delta_L} = \frac{(\lambda_m)^2 A_L \Delta T_m}{\rho_m c_m d\delta_L (d\delta)^2} \quad (8)$$

$A_L = Ld\delta$, $d\delta_L$ is the thickness of the infinitesimal heat conduction layer along the vertical direction of L .

The rising temperature of $A_L d\delta_L$ is:

$$\Delta T_{mL} = \frac{Q_{mL}}{\rho_m c_m A_L d\delta_L} = \frac{(\lambda_m)^2 \Delta T_m}{(\rho_m)^2 (c_m)^2 (d\delta_L)^2 (d\delta)^2} \quad (9)$$

Similarly, the heat transfer power equation along the vertical direction of W is:

$$Q_{mW} = \frac{(\lambda_m)^2 A_W \Delta T_m}{\rho_m c_m d\delta_W (d\delta)^2} \quad (10)$$

$A_W = Wd\delta$, $d\delta_W$ is the thickness of the infinitesimal heat conduction layer along the vertical direction of W .

The rising temperature of $A_W d\delta_W$ is:

$$\Delta T_{mW} = \frac{(\lambda_m)^2 \Delta T_m}{(\rho_m)^2 (c_m)^2 (d\delta_W)^2 (d\delta)^2} \quad (11)$$

In the theoretical model, the heat continues to transfer along the above directions, and each subsequent infinitesimal heat conduction layer has the above three directions of heat conduction. However, considering there is a huge difference in volume between the material and the MTEG unit, the contact between the MTEG unit and the material can be equivalent to that between the MTEG unit and a semi-infinite plate. While in the contact of the semi-infinite plate, only a part of the material has a temperature change, and the rest remains unchanged [20]. The effect of subsequent heat conduction on the results can be ignored since the temperature is unchanged. Therefore, only the heat transfers through the three directions mentioned above are calculated.

Therefore, the heat absorption power of the material is:

$$Q_{sum} = Q_m + Q_{m1} + Q_{mL} + Q_{mW} \quad (12)$$

The Q_{sum} comes from the cold end of the MTEG unit. According to the

first law of thermodynamics, the cold end releases the same heat as Q_{sum} . The cold end temperature drops as a result of the heat release, and the dropping temperature satisfies the equation:

$$\Delta T_{cool} = -\frac{Q_{sum} - Q_B}{\rho_{cool} c_{cool} A \delta_{cool}} \quad (13)$$

The subscript *cool* represents the cold end of the MTEG unit.

The variation of the cold end temperature changes the temperature difference of the MTEG unit. And through the MTEG unit, the temperature difference is converted into a voltage, which satisfies the equation:

$$V = S (T_{hot} - T_{cool}) \quad (14)$$

S represents the Seebeck coefficient of MTEG, and the subscript *hot* represents the hot end of the MTEG unit.

Finally, the relationship between thermal conductivity and voltage is obtained:

$$\Delta V = \frac{S(\lambda_m \delta_B (t_{m1} - t_{m2}) (A(\rho_m)^2 (c_m)^2 d\delta_L d\delta_W (d\delta)^2)}{\rho_{cool} c_{cool} A \delta_{cool} (\rho_m)^2 (c_m)^2 d\delta_L d\delta_W (d\delta)^3 \delta_B} + \frac{S \lambda_m \rho_m c_m A d\delta_L d\delta_W}{\rho_{cool} c_{cool} A \delta_{cool} (\rho_m)^2 (c_m)^2 d\delta_L d\delta_W (d\delta)^3 \delta_B} + \frac{S \lambda_B A_B (t_{shot} - t_{scool}) ((\rho_m)^2 (c_m)^2 d\delta_L d\delta_W (d\delta)^3 \delta_B)}{\rho_{cool} c_{cool} A \delta_{cool} (\rho_m)^2 (c_m)^2 d\delta_L d\delta_W (d\delta)^3 \delta_B} \quad (15)$$

In the Eq. (15), λ_B , A_B , ρ_{cool} , c_{cool} , A , δ_{cool} , δ_B , and S are all built-in parameters of the MTEG unit and the PU. $t_{B,hot}$ and $t_{B,cool}$ are the temperatures of the MTEG unit's hot end and cold end. After setting the experimental conditions, the above parameters are invariants. In addition, although the fact $(t_{m1} - t_{m2})$ gradually decreases after the device contacts the material, the variation can be ignored because of the short-term experiments. Therefore, the variables that affect ΔV are $d\delta_L$, $d\delta_W$, $d\delta$, ρ_m , c_m and λ_m . Because of the size difference, the influence between MTEG unit and material can balance each other. Hence $d\delta_L$, $d\delta_W$, $d\delta$, ρ_m , c_m can be ignored. Finally, ΔV is exclusively related to λ_m , which is the inherent property of the material itself.

Therefore, it is feasible to distinguish different materials by the variation of voltage. Besides, according to the Eq. (15), the built-in

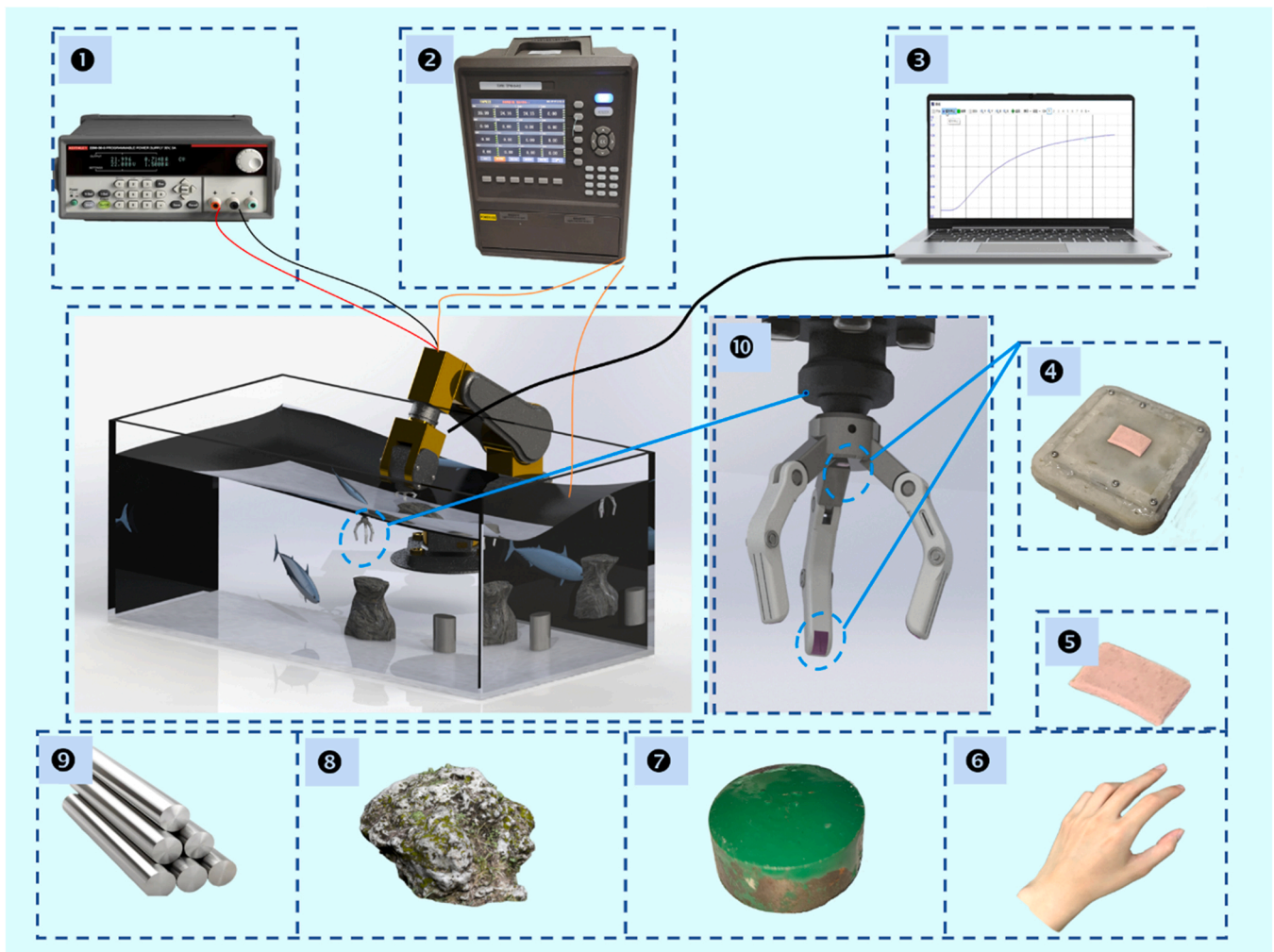


Fig. 4. Experimental system 1. the DC power source, 2. the data acquisition device, 3. the monitoring terminal, 4. the prototype, 5. the heat transfer enhancement module 6. human body, 7. marine steel with paint coating, 8. reef, 9. marine steel, 10. manipulator.

parameter S of the MTEG unit can also affect ΔV . By optimizing the MTEG unit to improve S , the variation of voltage can be more obvious, and the effect of material recognition can be improved.

Based on the above theoretical model, while the contact surface between the cold end of the MTEG unit and the material is non-ideal, the contact area A in Eq. (15) is no longer an invariant. Thus, the independent variable for ΔV increases to two independent variables, which are contact area A and material's thermal conductivity λ_m . In practice, the contact surface is usually non-ideal. Hence, recognition errors may happen due to the variation of contact area A caused by non-ideal contact surface. This conclusion is also verified in the following experimental studies. The flexible contact surface is employed to reduce the impact of contact area A on the recognition results. As seen in Fig. 2(d) and (e), the presence or absence of a flexible contact surface has a significant effect on thermal resistance.

The prototype and working principle are shown in Fig. 3. The prototype can be divided into the temperature control module, the MTEG module, and the heat transfer enhancement module three parts respectively. Among the three parts, the temperature control module corresponds to the PU in the theoretical model and the MTEG module corresponds to the MTEG unit in the theoretical model. The MTEG module is produced as a function of the thermoelectric effect, as shown in Fig. 3(a). When there is a temperature difference between the n-type semiconductor and the p-type semiconductor, the electrons are activated to transfer. With the transfer of electrons, a difference of electric

potential occurs between the cold end and hot end. As shown in Fig. 3(b), the sensitivity of the recognition module is approximately 72 mV/K.

The schematic of the prototype is shown in Fig. 3(c) and (d). The real photograph of the prototype is shown in Fig. 3(e) and (f). From top to bottom, the prototype is composed of the temperature control module, the MTEG module, and the heat transfer enhancement module. The prototype is wrapped with nylon fiber, which is robust and waterproof for adapting to the underwater environment. The temperature control module is utilized to maintain the hot end temperature of the MTEG module constant, and the MTEG module is utilized to recognize the material by feeding back voltage curves to the monitoring terminal. The heat transfer enhancement module, composed of the flexible contact surface, is utilized to optimize the recognition accuracy. The flexible contact surface is made of a material with both thermal conductivity and flexibility. The thermal conductivity exceeds 7 W/(m·K), the elastic modulus is 0.52Mpa, and the maximum compression ratio is 0.37. The prototype size is smaller than 40 mm × 40 mm × 60 mm to ensure the easy installation of the prototype in the manipulators.

3. Experiments and analysis

A series of experiments are performed to verify the theoretical model and test the performance of the prototype. Considering the potential heat source of the device, the heat source temperatures are set at 309 K and 323 K. Among them, 309 K is set to simulate the temperature of

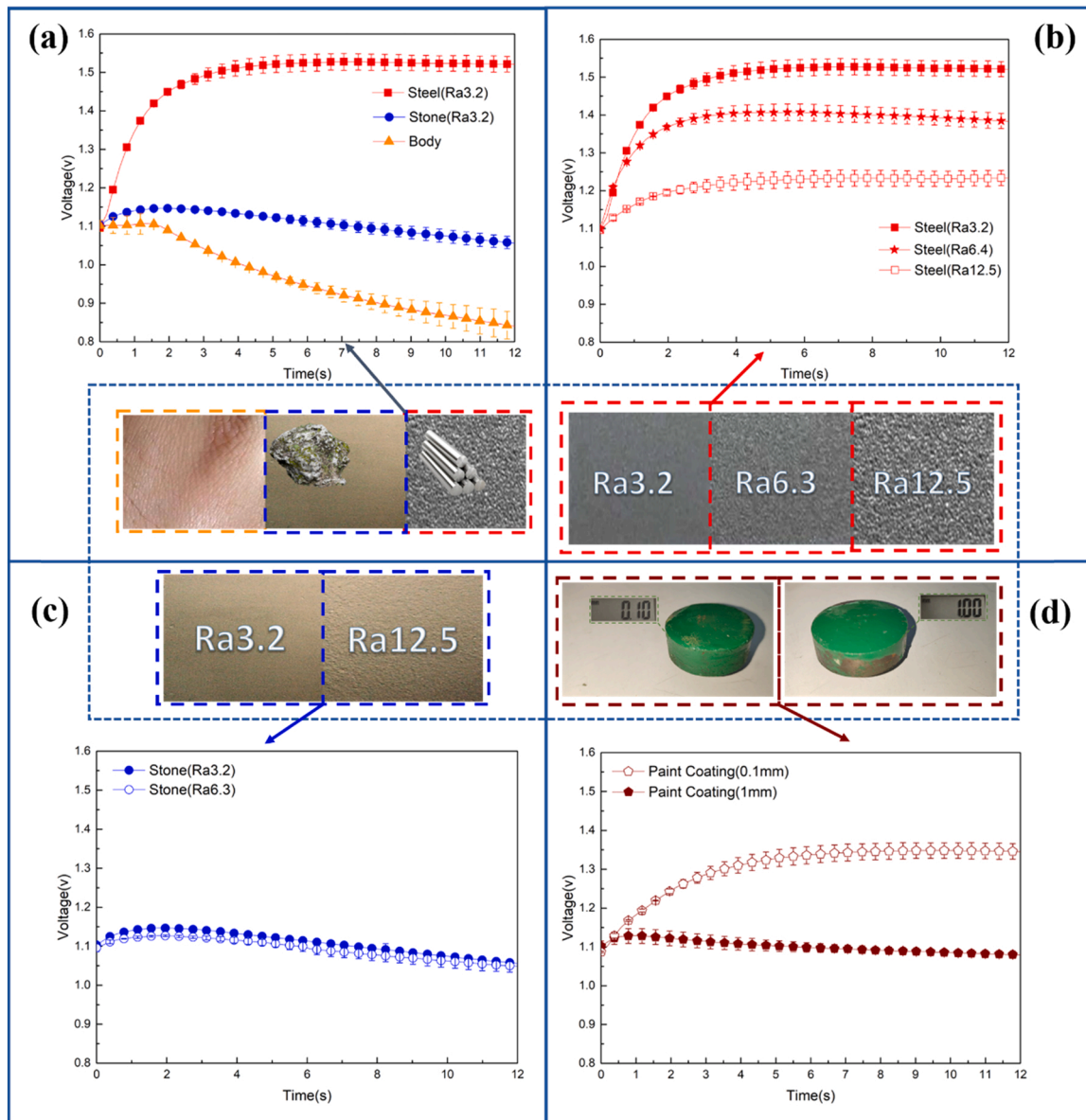


Fig. 5. The voltage curves under the condition of rigid contact with 309 K heat source temperature (a) voltage curves of different materials (b) voltage curves of the reef with different surface roughness (c) voltage curves of marine steel with different surface roughness (d) voltage curves of marine steel with different paint thickness.

humans as the heat source, 323 K is set to simulate the temperature of the lithium battery pack as the heat source. Moreover, experiments at different temperatures can also examine whether the recognition results are identical under different working conditions. Depending on the application of the prototype, the recognized materials can be divided into three typical categories: thermostatic animals, non-metal materials and metal materials. Among them, the reef and marine steel are widely distributed in underwater salvage and underwater monitoring application, while the human is the focus of underwater rescue. Once these three types of materials can be recognized, it is enough to meet the demands of most underwater recognition scenarios. Besides, during the recognition marine steel, a group of experiments is added to detect whether the prototype can recognize the paint coating thickness of the marine steel surface.

The experimental system is shown in Fig. 4. In the experiment, the DC power source is employed to provide energy for the temperature control module. The function of the data acquisition system is to monitor the hot end temperature of the MTEG module. Once the temperature

displayed on the data acquisition system mismatches the set temperature, the DC power supply should be adjusted until the displayed temperature is within ± 1 K, close to the temperature setting in the experiment. The function of the monitoring terminal is to record the voltage curves obtained from the MTEG module. The experiments are carried out in a flume filled with water, and the temperature of the water is adjusted according to the demand of the experiments. Ideally, the prototype should be installed in the manipulator. But during the experiments, the prototype is moved manually to contact or separate from the object. The experimental process is shown in Video.1.

Supplementary material related to this article can be found online at [doi:10.1016/j.sna.2022.113503](https://doi.org/10.1016/j.sna.2022.113503).

Considering the application scenario of the prototype is underwater and the annual average temperature of the Pacific, the largest and most important ocean, is 292.1 K. Moreover, the annual average water temperature at a depth of 1000 m is 277–278 K and the seawater temperature decreases with the depth. Assuming the prototype works at a depth of 100 m in the Pacific Ocean, the water temperature is set at about

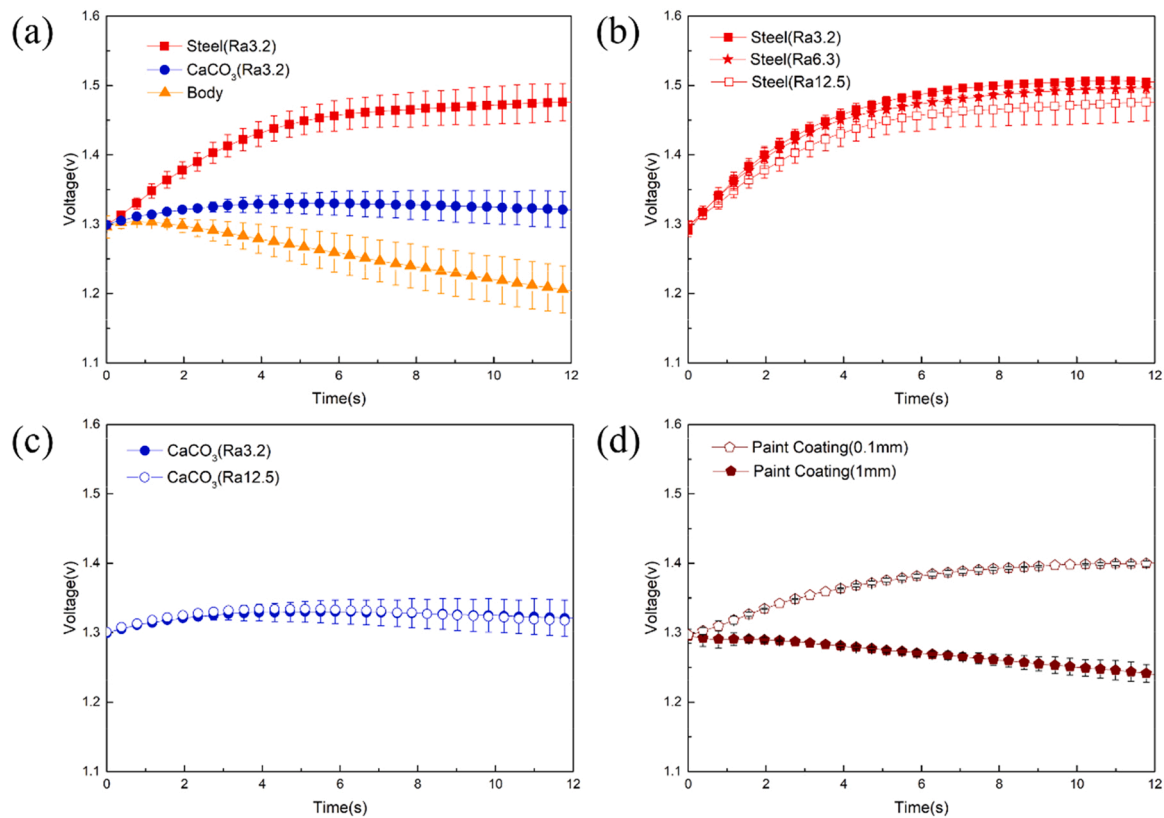


Fig. 6. The voltage curves under the condition of flexible contact with 309 K heat source temperature (a) voltage curves of different materials (b) voltage curves of the reef with different surface roughness (c) voltage curves of marine steel with different surface roughness (d) voltage curves of marine steel with different paint thickness.

283 K [19].

According to the existing research, a smooth or rough contact surface greatly affects the recognition effect of thermal tactile recognition [20]. The theoretical model proposed in this paper also makes it clear that the contact area can influence the recognition effect. Therefore, this paper also studies the influence of surface roughness on the recognition effect. When selecting the material, the same material with different surface roughness is selected. For example, when selecting marine steel, marine steel with surface roughness of Ra3.2, Ra6.3 and Ra12.5 is selected. The larger the Ra coefficient, the rougher the surface. Among them, the marine steel of Ra3.2 is utilized to represent the marine steel that has not been eroded by seawater. The marine steel of Ra6.3 is utilized to represent the marine steel eroded by seawater. The marine steel of Ra12.5 is clearly visible with various bulges and is utilized to represent the marine steel which has been eroded by seawater for a long time. In addition to materials selection, several groups of comparative experiments are carried out, which can be divided into rigid contact groups and flexible contact groups. The difference between the two groups is whether the flexible contact surface is added to the prototype. The flexible contact surface can theoretically reduce the influence of rough contact surface on recognition. The purpose of these experiments is to study whether the flexible contact surface can optimize the recognition effect. Due to the flexibility of biological skin, the influence of biological skin surface roughness on recognition can be ignored, so no comparative experiment is conducted on humans.

(1) Experimental data and analysis of heat source temperature sets at 309 K:

3.1. Rigid contact groups

Fig. 5 is the voltage curves under rigid contact with the heat source temperature at 309 K. It can be seen from Fig. 5(a) that the voltage

curves recorded by prototype after contacting the human, reef and marine steel have obvious characteristics respectively. Because the thermal conductivity of marine steel exceeds that of water, the heat transfer at the cold end of the MTEG unit is strengthened, resulting in the temperature drop of it. Therefore, the temperature difference between the cold and hot ends of the MTEG unit increases, and the voltage curves rise. While the cold end of the MTEG unit drops to a certain temperature, the heat transfer reaches an equilibrium, and the voltage curves tend to be parallel. The thermal conductivity of the reef is slightly inferior to that of water. Therefore, when the prototype just contacts the reef, though the water disturbance leads to a slight rise in the voltage curves, the voltage curves decline soon after the water disturbance subsides. As for human, though the thermal conductivity of human is not much different from that of water, human is a kind of constant temperature animal, and the temperature of the human body is almost the same as that of heat source. The temperature difference between the cold end and the hot end decreases rapidly, and the voltage curves also decline significantly. In the descending order of the voltage curves of three types of materials is marine steel > reef > human, and in the order of the voltage peak value is marine steel > reef > human. And it can be seen from Fig. 5(a) that when the time is at 2 s, the difference between the voltage curves of three types of materials is enough for recognition. Therefore, in the condition of heat source temperature at 309 K, the prototype can recognize different materials by comparing the voltage curves.

As shown in Fig. 5(b) and (c), the voltage curves of marine steel with a different surface roughness all gradually rise to a certain limit value and then tend to be stable. The voltage curves of the reef with different surface roughness both first slightly rise due to water disturbance, and then show a downward trend. However, the voltage curve of the same material varies with changes in the surface roughness. The roughness of the material affects the voltage curves, and the higher the thermal

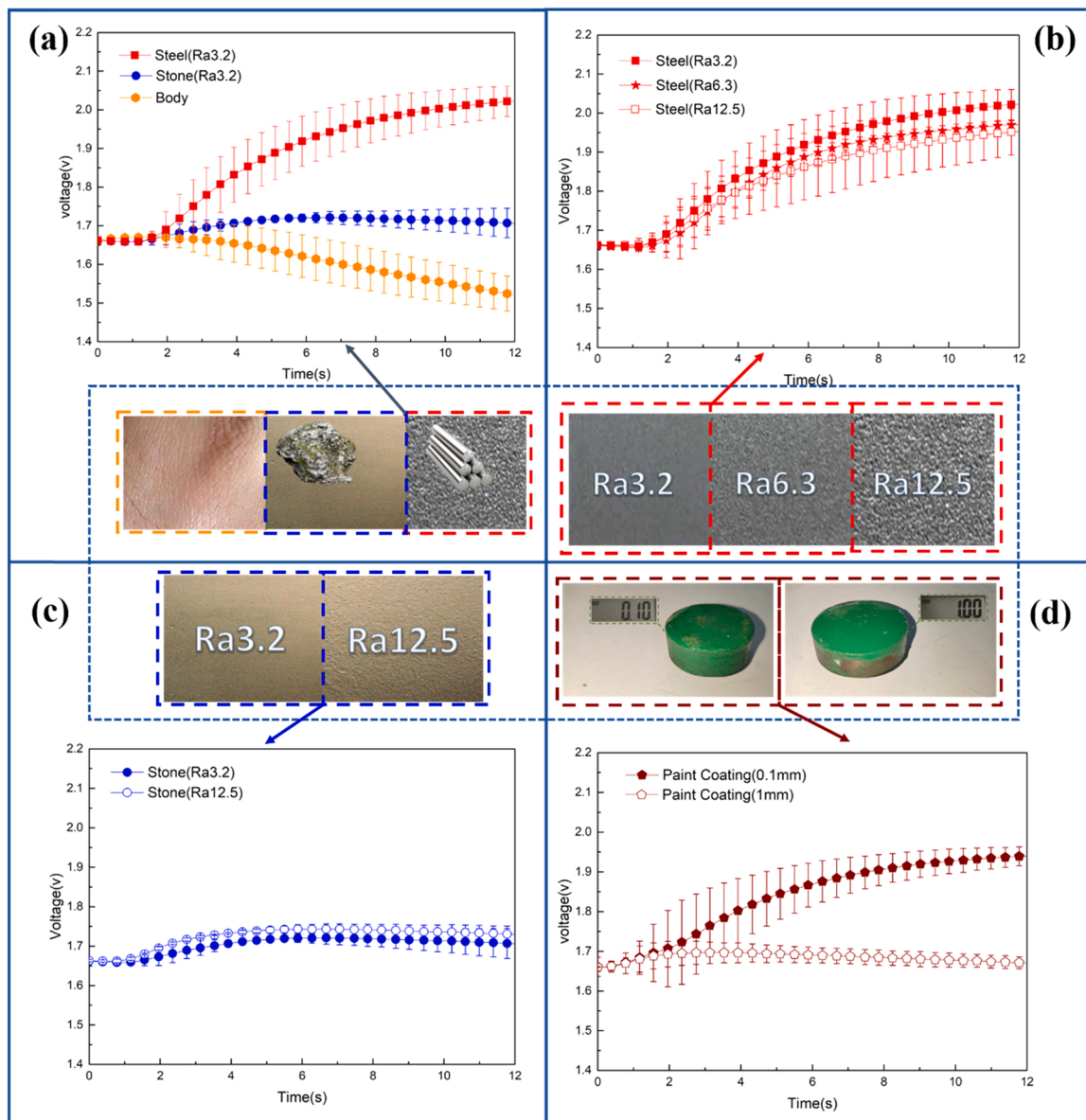


Fig. 7. The voltage curves under the condition of flexible contact with 323 K heat source temperature (a) voltage curves of different materials (b) voltage curves of the reef with different surface roughness (c) voltage curves of metals with different surface roughness (d) voltage curves of paint metals with different thickness.

conductivity of the material, the more obvious the variation is. Evidently, the variation leads to the decline of recognition accuracy.

It can be seen from Fig. 5(d) that the voltage curves reflect the thickness of the paint coating layer. Therefore, the thermal conductivity of the marine steel surface is affected after the paint coating is applied. Eventually, this causes the variation of the voltage curves. Once this phenomenon is regular and general, the voltage curves can be utilized to recognize the thickness of the marine steel surface paint coating. Specifically, it can be applied to the detection of ship paint. By applying this technology, robots can assist workers in doing hull detection.

3.2. Flexible contact groups

Fig. 6 is the voltage curves under flexible contact with heat source temperature at 309 K. It can be seen from Fig. 6(a) that the initial voltage value of voltage curves has increased compared to that in Fig. 5 (a). The reason is that after installing the flexible contact surface at the cold end of the MTEG unit, the heat transfer at the cold end is improved, so the initial temperature difference between the cold end and the hot

end of the MTEG unit is increased. With regard to marine steel and reefs, the difference in voltage value due to the difference in surface roughness is decreased. The reason is that the surface roughness has a positive correlation with the thermal resistance in the contact process. As for humans, the recognition voltage curves are slightly affected and are still in a rapid decline trend similar to those in Fig. 5(a). Although the three types of materials' voltage curves are all affected by the flexible contact surface, in the descending order of voltage curves is still marine steel > reef > human, and in the descending order of the voltage peak value is still marine steel > reef > human. The difference of three voltage curves is also obvious at about 2 s. Therefore, the flexible contact surface does not degrade the material recognition effect.

It can be seen from Fig. 6(b) and (c) that the variation among the voltage curves of the same material under different surface roughness conditions is significantly reduced. It indicates that the flexible contact surface can optimize the material recognition effect.

According to Fig. 6(d), after the prototype is installed with the flexible contact surface, the voltage curves of marine steel with different paint coating thicknesses are still significantly different, and the trend is

similar to that with rigid contact. Therefore, the flexible contact surface does not affect the possibility of recognizing the paint coating thickness on the marine steel surface.

3.3. Experimental data and analysis of heat source temperature sets at 323 K

Based on the optimization effect of the flexible contact surface on the prototype confirmed by the previous experimental results, the flexible contact surface is employed in the subsequent experiments.

Fig. 7 is the voltage curves in flexible contact with heat source temperature at 323 K. It can be seen from Fig. 7(a) that the voltage curves of the three types of materials are similar to those in Fig. 6(a). The voltage curves of marine steel are still stable after rising to a certain limit; the voltage curves of reef material are still parallel after an initial slight rise; the voltage curves of humans are still rapidly declining. In the descending order of voltage curves is still marine steel > reef > human, and in the order of the peak voltage value is still marine steel > reef > human. Obviously, the material recognition ability of the prototype is not affected by the variation of heat source temperature. It can be seen from Fig. 7(b) and (c), that for the same material, the voltage curves of different surface roughness remain within the acceptable error range. It means that the flexible contact surface can play an important role in optimizing recognition even when the temperature difference increases.

As shown in Fig. 7(d), the voltage curves of marine steel with different paint thicknesses are still different from each other, and the characteristics of the voltage curves are also significant. Therefore, this prototype is able to detect whether the bottom of the hull is rusty or attached by marine plants, which is a very promising application.

4. Conclusions

In this paper, a material recognition theoretical model based on the MTEG is proposed, and a prototype is designed to verify the theoretical model. The prototype can recognize thermostatic animals, non-metal materials and metal materials in approximately 2 s underwater. The prototype is compact in size, convenient in maintenance, and inexpensive. Besides, by applying the flexible contact surface, the recognition accuracy of the prototype is improved. In addition, the voltage curves recorded by prototype have an application prospect of recognizing the paint coating thickness of the marine steel. With the optimization of the MTEG and the enhancement of algorithm function, the material recognition device guided by this technology can not only recognize more types of materials, but also accurately recognize the proportion of different substances in materials.

Funding

This work is supported by the following funds: Fundamental Research Funds for the National Key R & D Project from Minister of Science and Technology (2021YFA1201604, Minyi Xu); Central Universities (Grants 3132019330, Changxin Liu); Innovation Group Project of Southern Marine Science and Engineering Guangdong Laboratory (Zhuhai) (No. 311021013, Minyi Xu); Natural Science Foundation of Liaoning Province of China (2020MS130, Zhitao Han).

CRediT authorship contribution statement

Changxin Liu: Conceptualization, Methodology, Supervision. **Bai-chuan shan:** Methodology, Writing – original draft. **Nanxi Chen:** Data curation, Formal analysis. **Jianhao Liu:** Data curation, software. **Zhenghui Zhou:** Software, Validation. **Qingyong Wang:** Formal analysis, Validation. **Yu Gao:** Validation. **Yunfei Gao:** Investigation. **Zhitao Han:** Investigation, Writing – review & editing. **Zhijian Liu:** Writing – review & editing. **Minyi Xu:** Writing – review & editing.

Declaration of Competing Interest

The authors declare that they have no known competing financial interests or personal relationships that could have appeared to influence the work reported in this paper.

References

- [1] Stefania, Matteoli, Marco, et al., ARTEMiDE—an automated underwater material recognition method for fluorescence LIDAR invariant to environmental conditions, *IEEE Trans. Geosci. Remote Sens.* (2020).
- [2] P. Alpizar, F. Bolanos, B. Rodriguez-Herrera, et al., An automatic acoustic bat identification system based on the audible spectrum, *Expert Syst. Appl.* (2014).
- [3] X. Wang, X.Q. Wang, J.Z. Sun, Study of target identification based on polarization imaging, *J. Yantai Univ. (Nat. Sci. Eng. Ed.)* (2007).
- [4] L. Zhou, Thermal tactile surface morphology identification, *Dongnan Daxue Xuebao (Ziran Kexue Ban)/J. Southeast Univ. (Nat. Sci. Ed.)* 40 (2010) 343–347.
- [5] D. Katz, L.E. Krueger, *The World of Touch*, Psychology Press, Hillsdale, N.J., 1989.
- [6] G. Havenith, Pain, thermal sensation and cooling rates of hands while touching cold materials, *Eur. J. Appl. Physiol. Occup. Physiol.* 65 (1992).
- [7] A.F. Mills, *Heat Transfe*, Second ed., CRC Press, 1999.
- [8] A. Sarda, R. Deterre, C. Vergneault, Heat perception measurements of the different parts found in a car passenger compartment, *Measurement* 35 (1) (2004) 65–75.
- [9] Xu D., Loeb G.E., Fishel J.A. Tactile identification of objects using Bayesian exploration[C]// IEEE International Conference on Robotics & Automation. IEEE, 2013.
- [10] Bhattacharjee T., Wade J., Kemp C. Material Recognition from Heat Transfer given Varying Initial Conditions and Short-Duration Contact[C]// Robotics: Science and Systems 2015. 2015.
- [11] Changxin Liu, Wenxiang Ye, Huanan Li, Jianhao Liu, Cong Zha, Zhuofan Mao, Xinxiang Pan, Experimental study on cascade utilization of ship's waste heat based on TEG-ORC combined cycle, *Int. J. Energy Res.* 45 (3) (2021) 4184–4196.
- [12] Changxin Liu, Huanan Li, Wenxiang Ye, Jianhao Liu, Huibin, Wang, Minyi Xu, Xinxiang Pan, Zhuofan Mao, Jiashuo Yang, Simulation research of TEG-ORC combined cycle for cascade recovery of vessel waste heat, *Int. J. Green Energy* 18 (11) (2021) 1173–1184.
- [13] Changxin Liu, Cong Zhao, Jianhao Liu, Jianye Wang, Yan Wang, Yuhang Fan, Kaiyuan Zhao, Baichuan Shan, Zhiyu Qu, Kefei Ma, Minyi Xu, Xinxiang Pan, Design and study of a combining energy harvesting system based on thermoelectric and flapping triboelectric nanogenerator, *Int. J. Green Energy* 18 (12) (2021) 1302–1308.
- [14] Changxin Liu, Fangming Li, Cong Zhao, Wenxiang Ye, Kaida Wang, Experimental research of thermal electric power generation from ship incinerator exhaust heat, *IOP Conf. Ser.: Earth Environ. Sci.* 227 (2) (2019), 22031–22031.
- [15] Changxin Liu, Xinxiang Pan, Xiaofeng Zheng Yuying Yan, Weizhong Li, An experimental study of a novel prototype for two-stage thermoelectric generator from vehicle exhaust, *J. Energy Inst.* 89 (2) (2015) 271–281.
- [16] C. Liu, J. Liu, W. Ye, et al., Study on a new cascade utilize method for ship waste heat based on TEG-ORC combination cycle, *Environ. Prog. Sustain. Energy* (2021), e13661, <https://doi.org/10.1002/ep.13661>.
- [17] W. Ye, C. Liu, J. Liu, et al., Research on TEG–ORC combined bottom cycle for cascade recovery from various vessel waste heat sources, *Arab. J. Sci. Eng.* (2021), <https://doi.org/10.1007/s13369-021-06050-3>.
- [18] Yang SM, Tao WQ. *Heat Transfer* (4th edition). 2006.
- [19] H. Wang, M. Ting, Covariabilities of winter U.S. precipitation and pacific sea surface temperatures, *J. Clim.* 13 (20) (2000) 3711–3719.
- [20] Chen Congyan, Shichen, et al., How the skin thickness and thermal contact resistance influence thermal tactile perception, *Micromachines* (2019).



Changxin Liu, received his PhD degree from Dalian University of Technology in 2014. Now he is a lecturer in the Marine Engineering College, Dalian Maritime University. His current research is mainly focused on the areas of blue energy, self-powered systems, compound energy harvesting, triboelectric nanogenerators, micro thermoelectric power generation and their practical applications in smart ship and ocean.



Baichuan Shan, is currently pursuing his master degree in Dalian Maritime University, China. His current research interests include Thermal tactile and bionic sensor.



Zhenghui Zhou, is currently pursuing his bachelor degree in Dalian Maritime University, China.



Nanxi Chen, is currently pursuing his master degree in Dalian Maritime University, China. His current research interests include thermal tactile and self-powered systems.

Qingyong Wang, is currently pursuing his bachelor degree in Dalian Maritime University, China.

Yu Gao, is currently pursuing his PhD degree in Dalian Maritime University.

Yunfei Gao, is a Teacher in Dalian Maritime University.

Zhitao Han, is a Professor in the Marine Engineering College, Dalian Maritime University.

Zhijian Liu, is a lecturer in the Marine Engineering College, Dalian Maritime University.



Jianhao Liu, is currently pursuing his master degree in Dalian Maritime University, China. His current research interests include blue energy harvesting and triboelectric nanogenerators.



Minyi Xu, received his PhD degree from Peking University in 2012. During 2016–2017, he joined Professor Zhong Lin Wang' group at Georgia Institute of Technology. Now he is a Professor in the Marine Engineering College, Dalian Maritime University. His current research is mainly focused on the areas of blue energy, self-powered systems, triboelectric nano-generators and its practical applications in smart ship and ocean.